Check for updates

Re-evaluating the role of phosphinic acid (DINHOP) adsorption at the photoanode surface in the performance of dye-sensitized solar cells

Manuel Rodríguez-Perez, [ID] [a] Felipe Noh-Pat,[a] Alfredo Romero-Contreras,[b]
Emigdio J. Reyes-Ramírez,[b] Siva Kumar Krishnan, [ID] [b] Jose L. Ortíz-Quiñonez, [ID] [b]
Joaquín Alvarado,[c] Umapada Pal, [ID] [b] Paul Olalde-Velasco [ID] [d] and
Julio Villanueva-Cab [ID] *[b]

Dineohexyl phosphinic acid (DINHOP) is a popular amphiphilic molecular insulator considered as the most efficient co-adsorbent (co-grafter) for the improvement of the photovoltaic performance of TiO$_2$ based hybrid solar cells. Although the effect of its incorporation on the improvement of cell performance has been well demonstrated, the mechanisms through which it affects the photovoltaic and electrodynamic parameters of the cells are not yet clear. Here we re-examine the mechanism through which the DINHOP co-adsorbent affects the photovoltaic and electrodynamic parameters of dye-sensitized solar cells. Although DINHOP is widely believed to inhibit (passivate) recombination across the TiO$_2$/electrolyte interface, we demonstrate that this is sublte, noticeable only for a very high concentration (*e.g.* 750 μM) of DINHOP, co-sensitized with a dye. For the most frequently used DINHOP concentrations (*e.g.* 75 μM and 375 μM), an observed increase of the diffusion coefficient and recombination rate could be directly associated with a decrease of total intra-gap states in TiO$_2$. For a DINHOP concentration as low as 75 μM, the conduction band edge of TiO$_2$ moves upward due to the combined effect of charge accumulation and a decrease in the total number of intra-gap states leading to an effective enhancement of the DCCS V_{OC}, where the decrease in total intra-gap states does not contribute positively. The decrease of total intra-gap states enhances both the transport and recombination rates of charge carriers by the same fraction due to a transport-limited recombination process. On the other hand, adsorption of DINHOP molecules at higher concentrations such as 375 μM and 750 μM additionally modifies the distribution of intra-gap states, affecting the nonlinear recombination parameter of charge carriers at the anode–electrolyte interface, leading to an overall enhancement of the DSSC V_{OC}. In all cases, incorporation of DINHOP results in an overall improvement of the solar cell efficiency (∼14% compared with the reference one), with a maximum for a concentration of 375 μM, where no inhibition of recombination was observed. Interestingly, for this DINHOP concentration, we estimate that 1 DINHOP molecule per every 12 molecules of dye occupies the intra-gap states of the TiO$_2$ surface. The results presented in this work elucidate the physical phenomena involved in the interaction of co-adsorbents, pre-treatments or additives with the electrolyte at the surface of the TiO$_2$ photoanode of dye-sensitized solar cells and can be easily adapted to study other electrochemical systems.

[a] *Facultad de Ingeniería, Universidad Autónoma de Campeche, Campeche, Campeche, Mexico*

[b] *Instituto de Física, Unidad Ecocampus-Valsequillo, Benemérita Universidad Autónoma de Puebla, Apdo. Postal J-48, Puebla, Puebla 72570, Mexico. E-mail: juliovc@ifuap.buap.mx*

[c] *Centro de Investigación en Dispositivos Semiconductores, Instituto de Ciencias, Benemérita Universidad Autónoma de Puebla, Apdo. Postal J-48, Puebla, Puebla 72570, Mexico*

[d] *Diamond Light Source Ltd., Harwell Science and Innovation Campus, Didcot OX11 0DE, UK*

Introduction

Sensitized nanostructured solar cells are promising photo-electrochemical devices for efficient, low-cost solar-to-electrical energy conversion. Dye-sensitized solar cells (DSSCs) have achieved conversion efficiencies beyond 11% under full sunlight (AM 1.5 solar irradiance)[1,2] and an extraordinary 32% with indoor light (1000 lux).[3] While the fabricated DSSCs show high short-circuit photocurrent and good fill factors, their open circuit voltages V_{OC} are substantially lower than theoretically predicted values.[4,5] The open circuit photovoltage of a DSSC is

determined by the difference between the electron quasi-Fermi level of TiO$_2$ in the active electrode under illumination (E_F) and the Fermi level (redox level) in the dark (E_{ref}).[6] A major factor limiting the V_{OC} of TiO$_2$ photoanode-based DSSCs is the back reaction transfer (recombination) of electrons, occurring from the TiO$_2$ photoanode to the redox electrolyte. However, changing the rate of charge carrier recombination, the redox potential level and/or the band edge position of TiO$_2$, it is possible to tune the photovoltage of these cells (DSSCs).[7–17]

Several strategies of surface treatment have been employed to either suppress the charge recombination in TiO$_2$ photo-anodes, or to shift its conduction band edge upwards (towards more negative potential), in order to enhance the V_{OC}.[7–17] Among them, the use of a co-adsorbent has been very effective. The co-adsorbents can be incorporated simultaneously with dye molecules over the semiconductor surface of DSSCs, which occupy the sites over the semiconductor surface uncovered by dye molecules to suppress charge recombination[18–21] Most of the co-adsorbents are organic amphiphilic molecules containing anchoring groups such as –COOH, –H$_2$PO$_3$, –SO$_3$H, etc.

Zhang et al.[18] have demonstrated the use of 4-guanidinobutyric acid (GBA) as a co-adsorbent dye in DSSCs fabricated with nanocrystalline TiO$_2$ and an amphiphilic ruthenium sensitizer. The use of GBA as a co-adsorbent not only helps in sealing the TiO$_2$ surface, but also inhibits the charge (electron) transfer from TiO$_2$ to the triiodide in the electrolyte, resulting in a shift of the quasi-Fermi level of TiO$_2$ and an increase of the open-circuit voltage by 50 mV. On the other hand, Ren et al.[20] demonstrated that the use of different cationic co-adsorbents affects the charge recombination and conduction band edge movement in different ways. Using two cholic acid (CA) co-adsorbents such as deoxycholic acid (DCA) and sodium deoxycholate (DCNa), they found that while DCA shifts the CB positively by 26 mV and retards the charge recombination by 10 fold, DCNa shifts the conduction band edge negatively by 33 mV and retards charge recombination by 3 fold, resulting in a V_{OC} gain of 41 mV and 65 mV, respectively.

Amphiphilic co-adsorbents, grafted onto the surface of TiO$_2$ in combination with a sensitizer, have been utilized to improve the V_{OC} of TiO$_2$-based DSSCs.[7–17] An amphiphilic co-adsorbent such as DINHOP has been reported to induce an upward shift (towards negative potential) of the conduction band edge of TiO$_2$, along with suppressing the interfacial recombination of photogenerated charge carriers,[11] offering the best scenario for enhancing the V_{OC} of a DSSC.

The phosphinic group of DINHOP is believed to bind with titanium ions at the TiO$_2$ surface, leaving the two neohexyl substituents attached to phosphinic acid as a hydrophobic insulating buffer between the TiO$_2$ photoanode and the electrolyte (Chart 1).[11] The effect of different co-adsorbents on a used dye, such as D29, has been studied by Rensmo et al.[22] They demonstrated that the used co-adsorbents such as DPA (decyl-phosphonic acid), DINHOP and CDCA (chenodeoxycholic acid) with the D29 dye have different performances. While DPA, containing a double phosphonic acid group, bound more efficiently to the TiO$_2$ surface in comparison to DINHOP, both
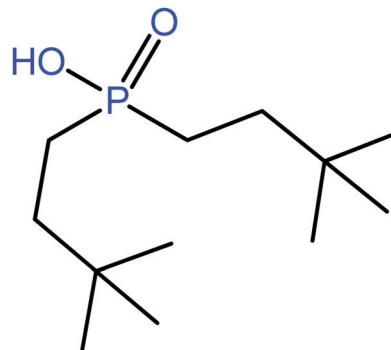

Chart 1 Chemical structure of dineohexyl phosphinic acid (DINHOP). Due to the difference in the electronegativity of the phosphorus atom (2.17) and the oxygen atom (3.5), they form an electric dipole, which favours the adsorption of DINHOP molecules at the titanium cation sites (oxygen vacancies) of the TiO$_2$ surface.

reduce the surface coverage of dye molecules, decreasing the photocurrent response of the fabricated devices. Very recently Chandiran et al.[23] have studied the effects of different functional groups of co-adsorbents and adsorbents, such as carboxylic (4-guanidino butyric acid and chenodeoxycholic acid), phos-phinic (dineohexyl phosphinic acid), and phosphonic (dodecyl phosphonic acid) groups, co-grafted with a hydrophobic Ru-based dye (C106) on the TiO$_2$ surface using ATR-FTIR spectroscopy, dye desorption and charge extraction measurements. They concluded that DINHOP is a true co-adsorbent, whose molecules replace dye molecules from their binding sites of dye-adsorbed TiO$_2$ photoanodes, rather than filling the free-space between the dye molecules. They reported an upward shift of trap-states only for optimum DINHOP concentration, which led to an enhancement of open circuit voltage, without providing information on other DINHOP concentrations. Nor did they discuss the effect of DINHOP concentration on the carrier recombination rate and diffusion coefficient. Although the use of DINHOP as a co-adsorbent has been reported to be beneficial in most of the cases,[11,23] the mechanisms through which the concentration of any co-adsorbent or adsorbent affect the TiO$_2$ surface, modifying the photovoltaic parameters of dye-sensitized solar cells, remained unclear. Attempts to improve DSSC performance are not limited to the use of co-adsorbents; novel dyes and electrolytes, electrolyte additives, etc. have also been tested and studied.[21,24,25]

In this work, we examine the effects of DINHOP adsorbed at the surface of TiO$_2$ electrodes over the open circuit voltage and electrodynamic parameters (transport and recombination) of DSSCs, using a small perturbation technique such as Stepped Light-Induced Transient Measurements (SLITM), a technique used to obtain electrodynamic parameters of TiO$_2$ photoanode-based DSSCs. The well-known total electron density model for DSSCs was used to interpret the obtained electrodynamic parameters to establish a direct relationship between micro-scopic (i.e. intra-gap states, electron diffusion at the conduction band edge, etc.) and macroscopic (photo generated electron charge density, V_{OC}, etc.) parameters. Specifically, we examine how the DINHOP concentration (co-grafted with Z907 dye) affects the conduction band edge of TiO$_2$, and transport and

carrier recombination kinetics, leading to an overall efficiency enhancement of a DSSC. For the first time, we distinguished two different contributions of DINHOP adsorbed at the TiO$_2$ electrodes: (1) surface passivation through a decrease in the total number of intra-gap states (N_{traps}) of TiO$_2$. The effect of N_{traps} decrease is manifested through the increase both in the diffusion coefficient and the recombination rate (transport-limited recombination), but does not contribute positively to the DSSC performance, and (2) surface passivation through the decrease of recombination rate constant k_0; this is a subtle feature, noticeable only for the higher concentrations of DIN-HOP molecules, associated with the insulating nature of their neohexyl groups. In all cases, incorporation of DINHOP results in an overall improvement of the solar cell efficiency, with a maxiumum of 7.4% for a concentration of 375 μM, mostly due to an upward shift of the conduction band edge without inhibition of recombination.

Experimental

Materials

TiO$_2$ paste (18NR-T), transparent conducting oxide (TCO) coated glass substrates (F-doped SnO$_2$; 15 Ω sq^{-1}), thermoplastic (Surlyn, Dupont grade 1702), and Z907 dye were purchased from Greatcell. 1-Butyl-3-methylimidazolium iodide, iodine, acetonitrile and valeronitrile were purchased from Sigma-Aldrich. Dineohexyl phosphinic acid (DINHOP) was synthesized as described in the literature.[11]

Device fabrication

TiO$_2$ films of about 0.25 cm^2 area were fabricated by depositing the TiO$_2$ paste (18NR-T) onto a TCO-coated glass substrate through screen-printing. After air-drying, the deposited layers were sintered in air at 500 °C for 1 h. The average thickness (d) of the fabricated nanocrystalline TiO$_2$ layers was about 12 μm (measured by a Dektak II profilometer). While cooling, the films were taken out of the annealing furnace at 80–100 °C, and immersed in a acetonitrile/*tert*-butyl alcohol (1:1, v/v) solution containing 0.375 mM Z907 dye + X μM of the co-adsorbent DINHOP (with X = 0, 75, 375 and 750) for 16 h. Semi-transparent counter electrodes were prepared by spreading two drops of 5 mM H$_2$PtCl$_6$ solution (in 2-propanol) over TCO-coated glass substrates and their subsequent firing at 450 °C for 1 h. The electrode (TiO$_2$ film + Z907 dye + DINHOP) and Pt-covered counter electrode were then sandwiched together using a 25 μm thick thermoplastic (Surlyn, Dupont grade 1702). After introducing the electrolyte solution into the sandwiched electrodes, the predrilled holes of the counter electrode were sealed with small pieces of corning glass using the thermoplastic. The electrolyte used in the DSSCs contained 0.6 M 1-butyl-3-methylimidazolium iodide and 0.03 M iodine in acetonitrile/valeronitrile (85:15, v/v%).

Device characterization

Fabricated devices were characterized at room temperature using a 450 W ozone-free Xe-lamp (LOT-Oriel) with a water filter calibrated to an irradiance of 100 mW cm^{-2} (equivalent air mass AM 1.5G) at the surface of the solar cell as illuminating source. The intensity of illumination at the surface of the devices (DSSCs) was calibrated using a certified 4 cm^2 mono-crystalline silicon reference cell with an incorporated KG-5 filter. No mask was used during the photovoltaic characterization of the DSSCs.

The SLITM of photovoltage and photocurrent is a small perturbation technique similar to IMPS (intensity modulated photocurrent spectroscopy), IMVS (intensity modulated photo-voltage spectroscopy) or EIS (electrochemical impedance spectroscopy) frequently used to measure the electrodynamic properties (*e.g.* charge transport and recombination) of DSSCs.[26,27] In fact, all these three techniques provide similar information on the electrodynamic parameters of an assembled DSSC. For SLITM measurements, the DSSCs were probed with a steeped modulated laser-LED beam of 630 nm wavelength (probe) superimposed on a relatively large background (bias) illumination, which is also a 630 nm laser-LED beam (bias). The probe and the bias laser lights enter the cells through the electrode side (TiO$_2$ coated conducting glass). The photovoltage decay due to probe light was recorded using a DPO70404 Tektronix oscilloscope, and fitted to a single exponential decay with exponent $-t/\tau_{rec}$, where τ_{rec} is the fitting parameter, termed as electron lifetime (or recombination time).[26,28] A similar procedure was followed to estimate the electron transport-time τ_t. However, in the latter case, the measurements were performed under short-circuit conditions while recording the photocurrent transient, and the obtained curves were fitted to single exponential decays using the exponent τ_t (electron transport-time).[26,28] Photovoltage (V_{OC}) and photocurrent (J_{SC}) at the corresponding applied bias were also recorded. The steady-state photoinjected electron density in the TiO$_2$ films was estimated from the relation $n = \alpha^{-1} J_{SC} \tau/(qd(1 - P))$,[29] where α is the measure of steepness of the intra-gap state distribution or the average trap depth,[30,31] J_{SC} is the short circuit photocurrent density established by the bias light, P is the film porosity (P = 0.6), q is the elementary charge ($|e|$), τ is the electron transport-time at short circuit or the electron lifetime under open circuit conditions, and d is the TiO$_2$ film thickness. Neutral density filters were used to vary the intensity of illumination, to generate plots of the electron recombination rate ($k = 1/\tau_{recombination}$), diffusion coefficient ($D = d^2/3.54\tau_{transport}$) and open circuit voltage, V_{OC}, as a function of electron charge density n. The open circuit voltage and short circuit current were recorded for each illumination intensity.

Theoretical considerations

Electron transport and recombination in DSSCs depend strongly on the intensity of illumination. Such intensity dependence of transport and recombination in a semiconductor has been attributed to the broad distribution of trap states inside its band gap.[6,26,28] The kinetics of charge transport in TiO$_2$ is a function of the electron density (or the quasi Fermi level), which has been
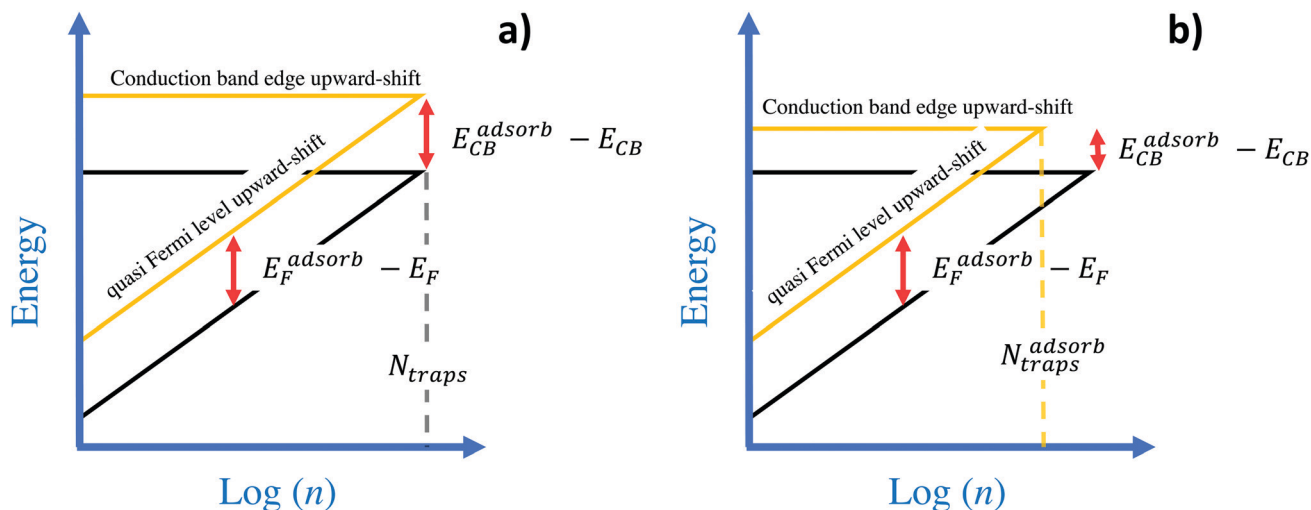
Fig. 1 Predicted shifts of the TiO$_2$ conduction band edge induced by negative charge of a co-adsorbent, (a) when the total number of intra-gap states is not affected the displacement on the quasi Fermi level, due to the co-adsorbent, is equal to the displacement of the conduction band edge (*i.e.* $E_F^{adsorb} - E_F = E_{CB}^{adsorb} - E_{CB}$), and (b) when the number of intra-gap states decreases the displacement on the quasi Fermi level, due to the co-adsorbent, is larger than the displacement of the conduction band edge (*i.e.* $E_F^{adsorb} - E_F > E_{CB}^{adsorb} - E_{CB}$), where N_{traps} represents the total intra-gap states below the conduction band edge and n the photogenerated charge density.

ascribed to the trap-limited transport process.[6,26,28] Electrons are reversibly trapped in and de-trapped from energy states (shallow and deep levels)[32] beneath the conduction band, and the de-trapping rate determines the transport kinetics.[6,26,28] The electrons in nanostructured TiO$_2$ films (n-type semiconductor) can be divided into two categories: conduction band electrons and trapped electrons. In nanostructured TiO$_2$ films, the majority of the photo-generated electrons remain trapped. The electron trap states remain distributed below the conduction band, and the density of electrons in them is assumed to be exponentially dependent on their energy with respect to the conduction band edge E_{CB} (Fig. 1). The distribution of electrons in the trap states can be expressed as a function of the quasi Fermi level E_F through the relation:[6,26,28]

$$n = N_{traps} \exp\left\{-\frac{\alpha(E_{CB} - E_F)}{kT}\right\} \quad (1)$$

where k is the Boltzmann constant, T the temperature and N_{traps} the total number of intra-gap states (shallow and deep levels). The open-circuit photovoltage, V_{OC}, of the DSSC is defined as the difference between the quasi-Fermi level E_F of eletrons in TiO$_2$ under illumination and the Fermi level in the dark E_{ref}:

$$V_{OC} = -\frac{E_F - E_{ref}}{q};$$
$$n = N_{traps} \exp\left\{-\frac{\alpha(E_{CB} - E_{ref} + V_{OC})}{kT}\right\} \quad (2)$$

Due to the Fermi level alignment equilibration, the position of the Fermi level of TiO$_2$ remains at the same level as that of the redox electrolyte in the dark.[6,26,28] For a constant charge density, the V_{OC} is fixed even if the recombination rate is modified by surface passivation of the TiO$_2$ layer. An exception of this occurs in the case of band-edge movement.[6]

Band-edge movement occurs when a sufficient number of negative or positive charges (or dipoles) build up at the surface of the TiO$_2$ particles to induce a change in the potential of their Helmholtz layer.[6,14,16,17] A negative surface charge built-up can cause the edges to shift upward, toward negative electrochemical potential, leading to a higher photovoltage. In contrast, a positive surface charge built-up can cause the conduction band edge to move downward, toward positive potential, favouring a lower photovoltage. However, all these are true when there is no change in the total intra-gap states of TiO$_2$, N_{traps}.[6,14,16,17,33]

The techniques used to demonstrate the band-edge movement are given elsewhere.[6,14,16,17] In brief, the band-edge movement in TiO$_2$ was monitored by comparing the dependence of V_{OC} on the photo-charge density (n) at open circuit induced by chemical treatment or adsorption of co-adsorbent at its surface (Fig. 1). The photo-charge density solely determines the difference between the conduction band edge and the quasi-Fermi level under illumination, following eqn (2). In the case of a fixed N_{traps}, a higher V_{OC} at a constant n indicates an upward movement of the conduction band edge; a lower V_{OC} at a constant n indicates a downward shift of the conduction band edge. As can be discerned from Fig. 1a, this shift can be mathematically expressed as $E_F^{adsorb} - E_F = E_{CB}^{adsorb} - E_{CB}$. In other words, the detected increase in V_{OC} at constant n due to the presence of a co-adsorbent at the TiO$_2$ surface can only be attributed to an upward shift of its conduction band edge by the same amount. On the other hand, it is well known that a chemical treatment or adsorption of foreign molecule (such as dyes, co-adsorbents, even the electrolyte solution) may modify the chemistry of the TiO$_2$ surface, leading to a change in surface charge and alteration of localized intra-gap states. All these modifications can be reflected in the photovoltaic and electrodynamic parameters of DSSCs.[6,33–36] As a consequence, if an adsorbent of negative charge is present at the TiO$_2$ surface affecting the total number

of intra-gap states N_{traps} we can deduct from Fig. 1b and eqn (1) a mathematical expression for the effective conduction band edge displacement:

$$\Delta E_{CB} = \Delta E_F - m_C \ln\{N_{traps}/N_{traps}^{adsorb}\} \tag{3}$$

where $\Delta E_F = E_F^{adsorb} - E_F$ and $\Delta E_{CB} = E_{CB}^{adsorb} - E_{CB}$. Consequently, using the $N_{traps}/N_{traps}^{adsorb}$ ratio in eqn (3), we can deduce the effective variation of the conduction band edge due to chemical treatment of the sensitized TiO$_2$ surface or due to the adsorption of a co-adsorbent. Likewise, the $N_{traps}/N_{traps}^{adsorb}$ ratio can be determined from the effect of a co-adsorbent on the charge density dependence of diffusion coefficient D, as presented below.

The diffusion coefficient of electrons in DSSC electrodes displays a power-law dependence with photoelectron density.[37–39] This nonlinear dependence has typically been attributed to multiple trapping and de-trapping of electrons during their transit through the nanostructured semiconductor film.[34,35,40–46] Within the framework of the exclusive random walk model, a relation between the diffusion coefficient D and the total electron density n has been derived as:[26,36,46,47]

$$D = D_0 \frac{N_c}{\alpha(N_{traps})^{1/\alpha}} n^{(1-\alpha)/\alpha} \tag{4}$$

where D_0 is a surface independent parameter and is related to the free electron mobility[48] and N_C is the density of states in the conduction band. The total intra-trap states in TiO$_2$ are believed to be associated with surface oxygen vacancies localized at the TiO$_2$ surface.[6] Consequently, a co-adsorbent at the TiO$_2$ surface can affect both its α and N_{traps}. Also, the effect can be verified by comparing the diffusion coefficient of electrons in the treated and untreated layers as a function of n. If the co-adsorbent does not affect the trap distribution parameter α, a decrease in N_{traps} can be understood as passivation through the intra-gap states, in agreement with eqn (3) and (4). Likewise, if the co-adsorbent does not modify either of α and N_{traps}, and also does not affect the electron diffusion coefficient, the passivation effect would be reflected as the change in V_{OC} at constant n in the V_{OC} versus log(n) plot, which can only be attributed to a shift of the conduction band edge.

On the other hand, knowing that electron diffusion to the intra-gap states controls recombination,[26,39] any attempt to improve the diffusion coefficient by decreasing the total trap density would result in an increase of the recombination rate k,[26,34] following the relation:

$$k = k_0 \frac{N_c^\beta}{(N_{traps})^{\beta/\alpha}} n^{(\beta-\alpha)/\alpha} \tag{5}$$

where k_0 is the recombination rate constant of free electrons, which is related to the microscopic mechanism of recombination, and β is the recombination reaction order with respect to free electrons (or the nonlinear recombination parameter), which depends on the nature of the TiO$_2$ surface, and can be varied due to modification by a co-adsorbent. Therefore, a sole decrease of k_0 can be understood as passivation through recombination kinetics. It is important to mention that the

recombination rate k (eqn (5)) accounts for all the recombination processes, which include recombination between the electron of TiO$_2$ and electron acceptors in the electrolyte (nongeminate) and recombination between electrons and oxidized molecules (geminate).

At this point, we can conclude that if the negatively charged molecules adsorbed onto the TiO$_2$ surface enhancing both the diffusion coefficient and the recombination rate by the same fraction (i.e. $\beta = 1$ and constant α) at constant charge density, the effect of surface passivation occurs through the decrease of total intra-gap states (eqn (3) and (4)). On the other hand, if the adsorbed molecule reduces the recombination rate k and increases the diffusion coefficient D, the effect can be understood as passivation through both the total intra-gap states and recombination kinetic (eqn (3)–(5)), the effect of which on the conduction band edge can be estimated from eqn (3). Likewise, if the co-adsorbent does not modify either the carrier transport or the recombination process, there occurs charge accumulation at the TiO$_2$ surface, which led to a shift (upward or downward depending on the nature of the charge) of the conduction band edge. Finally, the effect of a co-adsorbent on the surface of TiO$_2$ can be a combination of all the processes mentioned before, which in principle, could be monitored from the transport, recombination and voltage versus charge density plots, as we demonstrate below.

Results and discussion

To study the effect of the DINHOP co-adsorbent on the photovoltaic performance of DSSC electrodes, we used a DSSC with no DINHOP content as reference and DSSCs containing different amounts of the co-adsorbent (see Table 1). The reference cell exhibited J_{SC}, V_{OC} and fill factor (ff) values of 12.6 mA cm^{-2}, 755.9 mV and 66.6%, respectively, leading to a power conversion efficiency (PCE) of 6.3%. As can be observed in Table 1, in all cases, the use of the DINHOP co-adsorbent leads to an increase in J_{SC} up to 13.7 mA cm^{-2} for 75 μM concentration before dropping gradually on further addition up to 12.7 mA cm^{-2} for 750 μM, following a similar trend to that observed by Chandiran et al.[23] On the other hand, the V_{OC} also varied with the variation of the concentration of the co-adsorbent. A gradual increase from 755.9 mV to 790.3 mV was observed for the increase of DINHOP concentration up to 750 μM. As can be observed in Table 1, the ff also increases with the increase of DINHOP concentration, with a maximum value of 73.6% for 375 μM concentration of DINHOP. A maximum efficiency of 7.4% was

Table 1 Photovoltaic characteristics of DSSCs fabricated with TiO$_2$ photoanodes sensitized with Z907 (375 μM) solution and a neohexyl phosphinic acid co-adsorbent of different concentrations

DINHOP concentration (μM)	J_{SC} (mA cm^{-2})	V_{OC} (V)	FF (%)	E_{ff} (%)
0	12.6	755.9	66.6	6.3
75	13.7	766.9	68.6	7.2
375	13.0	771.8	73.6	7.4
750	12.7	790.3	72.3	7.3

obtained for the cell fabricated with a DINHOP concentration of 375 μM, mainly due to the increase in J_{SC}, V_{OC} and ff, resulting in an overall efficiency increase of around 14%. Such an increase in cell efficiency is in good agreement with the results obtained by Chandiran et al.,[23] who also noted the increase in J_{SC}, V_{OC} and ff to a possible (without proof) passivation of the TiO$_2$ electrode surface by the DINHOP co-adsorbent. Using FTIR and dye adsorption studies, they associated the observed decrease of J_{SC} at higher DINHOP concentrations to the replacement of dye molecules from binding sites by DINHOP molecules rather than filling the free-space between dye molecules. The variation of V_{OC} was explained in terms of an upward shift of the TiO$_2$ quasi Fermi level. In our case, we observed $\sim$9% increase in J_{SC} when 75 μm of DINHOP is used. The subtle increase of J_{SC} has been explained by Chandiran et al.[23] in terms of the ability of DINHOP molecules to align the dye molecules on the electrode surface, which favors the electron injection from their excited states. It is also important to mention that from the point of view of intermolecular forces, certainly there exist van der Waals forces between the neohexyl chains of DINHOP and the two nonyl chains of Z907 dye, which promote the de-aggregation of the dye molecules. Hence, it is possible that $(C_6H_{13})_2POO^-$ anions are formed and adsorbed at the TiO$_2$ photoanode surface. Therefore, the DINHOP could act both as co-adsorbent and dis-aggregating agent in a DSSC, as showed by Chandiran et al.[23] using dye desorption and AFTIR spectroscopy. Besides, the voluminous hydrophobic neohexyl chains of DINHOP can diminish the undesired attachment of the I_3^- anion to the TiO$_2$ surface, reducing the recombination of triiodide ions and electrons of the TiO$_2$ photoanode. As the Z907 dye used in this work and the C106 dye used by Chandiran et al.[23] differ only in the ancillary chains, it is reasonable to assume that the two dye molecules get adsorbed on the TiO$_2$ surface with a similar bond strength. Therefore, the variations of J_{SC} presented in Table 1 can be explained with similar arguments used by Chandiran et al.[23]

In the following sections, we will refer to DINHOP as a co-adsorbent even though it also has a de-aggregating property. As Chandiran et al.[23] did not provide electrodynamic aspects of DINHOP incorporation, we will discuss how the conduction band edge of TiO$_2$ and the transport and recombination kinetics of charge carriers are affected with the addition of the DINHOP co-adsorbent (co-grafted with the Z907 dye), leading to an overall efficiency enhancement, in comparison with the reference DSSCs fabricated without a co-adsorbent. The mechanism of surface passivation of TiO$_2$ due to DINHOP incorporation will also be discussed. It is important to mention that the electrodynamical analysis presented in this study can be generalized to study the effects of adsorbents, electrolytes, additives and other pre-treatments on the modification of TiO$_2$ and other metal oxide based photoanode surfaces.

Fig. 2 shows the variation of open circuit voltage, diffusion coefficient and carrier recombination rate with the variation of charge density for a DSSC containing 75 μM DINHOP co-adsorbent, in comparison with the reference DSSC (with no co-adsorbent). The lines in Fig. 2a represent the best fitting to eqn (2). Both the fitted lines revealed the same value of
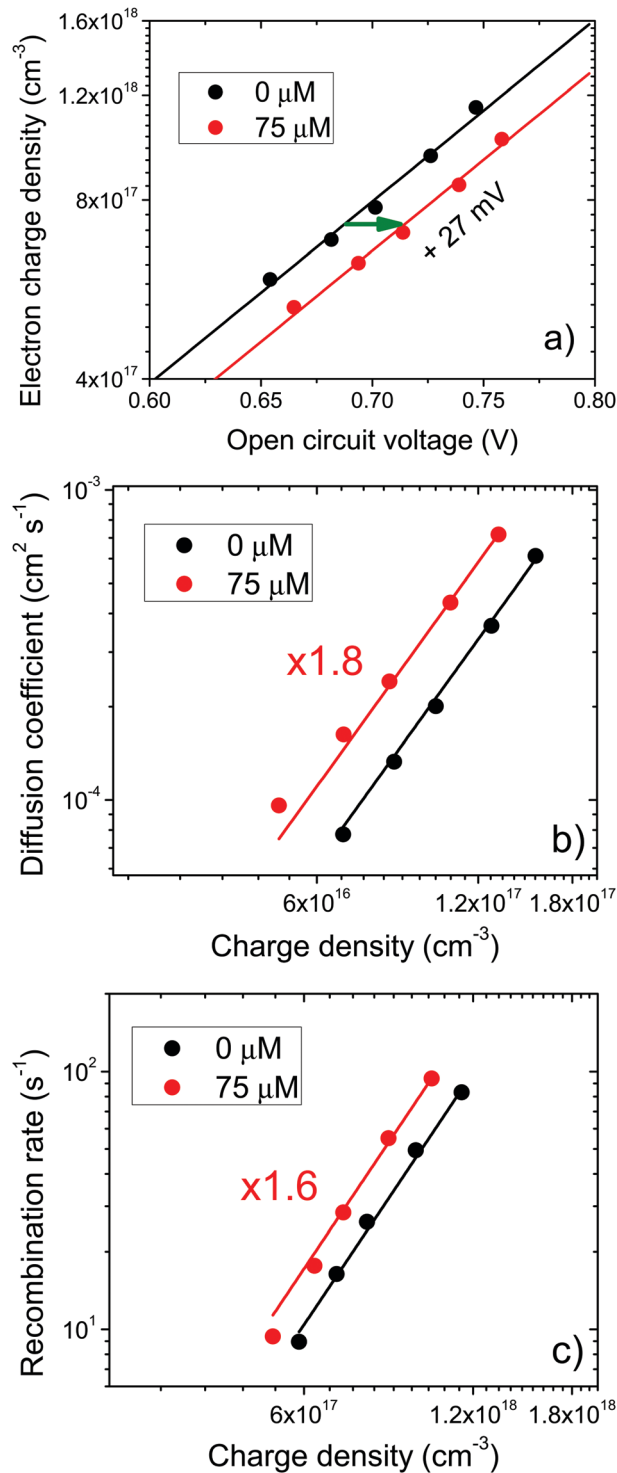

Fig. 2 Effect of 75 μM DINHOP co-adsorbed with the Z907 dye over a TiO$_2$ electrode. Variation of (a) the quasi Fermi level position (open circuit voltage), upward shift of 27 mV, (b) the diffusion coefficient, increased by a factor 1.8, and (c) the recombination rate with electron charge density, increased by a factor 1.6, for the assembled devices. The reference DSSC was the cell prepared with the TiO$_2$ film exposed just to the Z907 dye (375 μM).

α = 0.1832 (similar slopes in Fig. 2a) indicating that incorporation of a co-adsorbent at 75 μM does not significantly modify the distribution of intra-gap states of TiO$_2$. Fig. 2a also shows

that at constant n the V_{OC} of the cell increases by 27 mV due to DINHOP incorporation (75 μM). The increase of V_{OC} can be associated with an upward shift of the TiO$_2$ conduction band edge by about 27 mV, assuming that the total intra-gap states does not change on the incorporation of 75 μM DINHOP. As described earlier, this hypothesis can be tested by comparing the variations of transport (diffusion coefficient) and recombination (lifetime) parameters against electron charge density. Increases of both transport and recombination rate of electrons by the same fraction without changing α and β are the fingerprint of change in total intra-gap states due to the incorporation of a co-adsorbent onto the TiO$_2$ surface. As shown in Fig. 2b and c, due to adsorption of 75 μM of DINHOP, the diffusion coefficient and recombination rate of electrons increased by 1.8 and 1.6 fold, respectively. On the other hand (from the best fitting to eqn (4) and (5)), the non-linear recombination parameter ($\beta = 0.7785$) does not change significantly (similar slopes in Fig. 2c). Therefore, considering that the incorporation of DINHOP (with 75 μm concentration) modifies the total number of intra-gap states at the TiO$_2$ surface, and using the ratio of diffusion coefficients for the DSSCs with and without DINHOP, we can deduce the following relation from eqn (4):

$$N_{\text{traps}}/N_{\text{traps}}^{\text{adsorb}} = [D^{\text{adsorb}}/D]^{\alpha} \qquad (6)$$

where the superscript indicates the presence or the absence of DINHOP. Using eqn (6) and the values $D^{\text{adsord}}/D = 1.8$ (Fig. 2b) and $\alpha = 0.1832$ (Fig. 2a), we estimated a decrease of around 11% in the total intra-gap states due to incorporation of 75 μM DINHOP. Utilizing eqn (3) and the estimated change in intra-gap states (around 11%), an upward shift of about 12 meV of the conduction band edge (towards negative value) was estimated due to the incorporation of 75 μM DINHOP. On the other hand, using eqn (5) and a similar reasoning, we can deduce a mathematical relation to estimate the expected increase in the recombination rate due to the decrease of N_{traps}:

$$k^{\text{adsorb}}/k = [N_{\text{traps}}/N_{\text{traps}}^{\text{adsorb}}]^{\beta/\alpha} \qquad (7)$$

Utilizing the values of trap distribution ($\alpha = 0.1832$) obtained from Fig. 2a, the non-linear recombination parameter ($\beta = 0.7785$) obtained from Fig. 2c, and $N_{\text{traps}}/N_{\text{traps}}^{\text{adsorb}} = 1.11$ (obtained from Fig. 2b and eqn (6)) using eqn (7), we could estimate a 1.6 fold increase in the recombination rate due to the incorporation of 75 μM DINHOP, which agrees very well with the observed increase in the recombination rate constant for a fixed n (Fig. 2c). Therefore, we can conclude that the incorporation of 75 μM DINHOP co-adsorbent on the TiO$_2$ surface causes both a decrease in the total number of intra-gap states by around 11% and an upward shift of the conduction band edge by 12 meV. It must be noted that the estimated upward shift of the conduction band edge (12 meV) is very close to the 11 mV increase in open circuit voltage of the DSSC containing 75 μM of DINHOP (see Table 1). Therefore, the observed increase in V_{OC} due to the incorporation of the DINHOP co-adsorbent (75 μM) can be ascribed to the contributions of charge accumulation at the surface of TiO$_2$, and about 11% decrease in N_{traps}, without significant variation in the

recombination rate constant k_0, *i.e.* no passivation through the recombination path.

In the cases when 375 μM and 750 μM of DINHOP concentrations are used as co-adsorbents, the observed changes in the electrodynamic parameters of the cell were more dramatic in comparison with the electrodynamic parameters of the reference DSSC (Fig. 3). As can be observed in Fig. 3a, the subsequent increase in DINHOP concentration leads to a modification of intra-gap state distribution in TiO$_2$, followed by its saturation at 750 μM. The lines in Fig. 3a represent the best fittings to eqn (2) with $\alpha = 0.1377$ for both 375 μM and 750 μM concentrations. This result indicates that the increase in DINHOP concentration (from 75 μM) leads to an increase in the average number of deep intra-gap states below the conduction band edge of TiO$_2$. On the other hand, in Fig. 3b, we can observe that the diffusion coefficient increases with the increase of DINHOP concentration for a constant n. However, the change in the α value (with respect to the reference cell, black dots in Fig. 3b) is less noticeable compared with the one in Fig. 3a. Similar behaviour was observed by Pourjarafi *et al.* for their DSSCs fabricated with TiO$_2$ in the brookite phase obtained through different synthesis methods (acidic synthesis and basic synthesis with acidic treatment).[33]

For the sake of comparison, assuming a constant slope for all the DINHOP concentrations in Fig. 3b, we can estimate the variations of N_{traps} as a function of DINHOP concentrations (with respect to the reference DSSC). Using eqn (6) and the D^{adsord}/D values of 2.6 and 2.9 (obtained for the 375 μM and 750 μM DINHOP concentrations respectively, blue and olive dots in Fig. 3b), and $\alpha = 0.1377$ (obtained for both the 375 μM and 750 μM DINHOP concentrations, blue and olive dots in Fig. 3b), we estimate the decrease in N_{traps} values by 14% and 16% for the incorporation of DINHOP in 375 μM and 750 μM concentrations, respectively (compared to the reference DSSC). On the other hand, using eqn (6) and the values D^{adsord}/D values of 2.6 and 2.9 (obtained for the 375 μM and 750 μM DINHOP concentrations, respectively) and $\alpha = 0.1832$ (obtained for the reference DCCS, black dots in Fig. 3b), we could roughly estimate the decrease in N_{traps} values by 19% and 21% for the incorporation of DINHOP in 375 μM and 750 μM concentrations, respectively (compared to the reference DSSC). So, we can conclude that for 375 μM and 750 μM DINHOP concentrations, the N_{traps} value decreases by 14–19% and 16–21%, respectively. However, we could not apply eqn (3) to estimate the conduction band edge shift (ΔE_{CB}) for these cases (for DSSCs fabricated with 375 μM and 750 μM DINHOP concentrations) due to the variation in the α parameter with respect to the reference one. Fig. 3c compares the effect of DINHOP concentration on the carrier recombination rate in the DSSCs. As can be noticed, in comparison to the reference device (with no DINHOP), the recombination order parameter β of the DSSC fabricated with 375 μM DINHOP concentration decreases from 0.7785 to 0.7572 (considering the variation in $\alpha = 0.1832$ for the reference DSSC and 0.1377 for the DSSC containing 375 μM, eqn (6)). It is also interesting to note that for the highest DINHOP concentration (750 μM) no further variation of β was observed
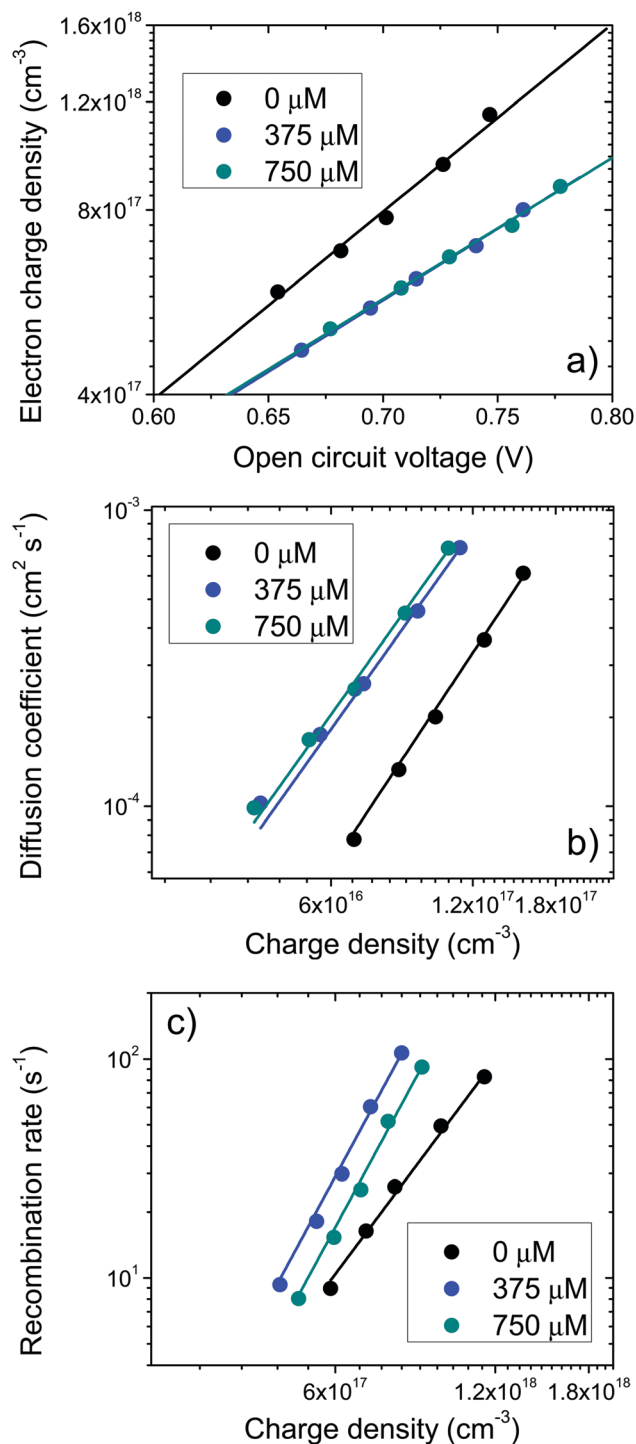
Fig. 3 Effect of 375 μM and 750 μM DINHOP co-adsorbed with the Z907 dye on the TiO$_2$ surface: (a) quasi Fermi level position (open circuit voltage), (b) diffusion coefficient and (c) recombination rate *versus* electron charge density for assembled devices. The reference DSSC is the cell fabricated with the TiO$_2$ film exposed only to the Z907 dye (300 μM).

(where $\alpha = 0.1377$ both for the DSSCs containing 375 μM DINHOP and 750 μM DINHOP).

Let us consider the sample with 375 μM of DINHOP as our new reference. From Fig. 3a, we can observe that on increasing the DINHOP concentration by a factor of two, no added

accumulation of negative charge (DINHOP) occurred at the TiO$_2$ surface, *i.e.* no change in the E_F occurred. On the other hand, no significant change in the value of diffusion coefficient (at constant n) could be observed (Fig. 3b). Using eqn (6), we obtained a small decrease in N_{traps} of around 1.5% due to the increase of DINHOP concentration from 375 to 750 μM. The significant difference between the latter two DINHOP concentrations (375 to 750 μM, blue and olive dots in Fig. 3c) is a 1.7-fold decrease in the recombination rate. So, from the point of view of the new reference (375 μM of DINHOP), the mechanism of passivation due to DINHOP incorporation turned out mainly through the recombination rate constant k_0.

The analysis presented above is in good agreement with results reported by Chandiran *et al.*[23] They conclude that the strong bonding of DINHOP molecules modifies the interfacial electrostatic dipole moment, moving the intra-gap states of TiO$_2$ upwards. Additionally, we demonstrate that a change in the total number of intra-gap states is also expected due to the incorporation of DINHOP at the surface of TiO$_2$, which can also be quantified from the analysis of transport and recombination kinetics against charge density plots. Interestingly, in contrast to the results reported by Chandiran *et al.*,[23] we could observe the passivation of the surface through charge recombination only for higher DINHOP concentrations (not for DINHOP concentrations lower than 750 μM). This is evident in the diffusion and recombination plots presented in Fig. 3b and c (blue and olive dots), where for the 750 μM concentration (olive dots), a decrease in the recombination rate is evident when compared with the new reference, 375 μM concentration (blue dots). It is important to mention that, due to the hydrophobic neohexyl chains of DINHOP, a decrease in the charge recombination rate is always expected for all the DINHOP concentrations. Inasmuch, due to the transport-limited recombination process, the effect of an increase in N_{traps} dominates in all the cases.

Fig. 4 shows the open circuit photovoltage *versus* short circuit photocurrent density for the DSSCs fabricated with TiO$_2$ electrodes sensitized by Z907 dye and co-sensitizer DINHOP of different concentrations at different light intensities. As can be observed, regardless of the DINHOP concentration, the variations of V_{OC} with J_{SC} (in a semi-logarithmic plot) are similar, and possess similar slope values. These plots show the overall effect of DINHOP concentration at several short circuit photocurrent densities.[16] For 75 μM DINHOP incorporation, the collective effects of charge accumulation over the TiO$_2$ surface causes an upward shift of the quasi Fermi level by about $\Delta E_F = 27$ mV, and a decrease in the total intra-gap states by 11%, which lead to a net increase of V_{OC} by about 11 mV (see Table 1 and Fig. 4). On the other hand, for 375 μM DINHOP incorporation, the collective effect of charge accumulation over the TiO$_2$ surface decreases in total intra-gap states, and the variation of their distribution leads to a net increase in V_{OC} by about 16 mV (see Table 1 and Fig. 4). Finally, for 750 μM of DINHOP incorporation, the collective effect of charge accumulation over the TiO$_2$ surface, the decrease in total intra-gap states, the variation of their distribution, and a decrease in the
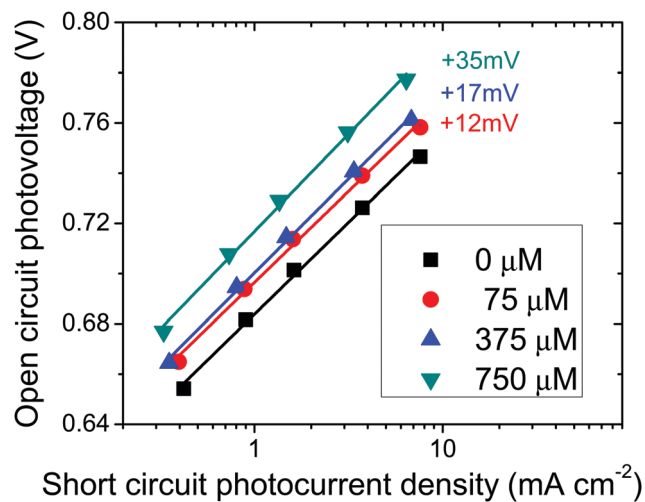
PCCP

Fig. 4 Open circuit photovoltage *versus* short circuit photocurrent density at different light intensities for Z907 dye co-sensitized with DINHOP at different concentrations. The reference DSSC is the cell prepared with the TiO$_2$ film exposed only to the Z907 dye (300 μM). The inset values (+12, +17 and +35 mV) are the enhanced V_{OC} values of DSSCs containing DINHOP of different concentrations.

recombination rate constant k_0 leads to a net increase in V_{OC} by about 34 mV (see Table 1 and Fig. 4). As has been stated earlier, negative charge accumulation at the TiO$_2$ surface due to DINHOP adsorption moves the conduction band edge upward, even solely dye adsorption moves the TiO$_2$ conduction band edge.[11] As the dye and DINHOP molecules compete with each other to get attached to the oxygen vacancies of the TiO$_2$ surface it is possible that in most of the cases, electrons from DIHNHOP molecules occupy the intra-gap states, leading to a decrease in N_{traps}, while at the same time get accumulated at the TiO$_2$ surface, *i.e.* moving the conduction band edge upwards at higher DINHOP concentrations, causing a modification of intragap states. As can be noticed, charge accumulation is the most important factor for the improvement of V_{OC} in DSSCs, neither the decrease of N_{traps} nor the variation of their distribution. It is also interesting to note that even though the effect of DINHOP adsorption at the TiO$_2$ surface is believed to avoid charge recombination through blocking by the hydrophobic chains of the co-adsorbent molecules, this effect was noticed only for higher concentrations (*i.e.* at 750 μM). Even for the mostly used concentration of 375 μM, the DINHOP molecules adsorbed over the TiO$_2$ surface were not enough to block the recombination path of electrons at the TiO$_2$–electrolyte interface.

It is illustrative to calculate the change in surface charge density ΔQ that would result in a 10 mV upward shift of the TiO$_2$ conduction band edge. From the Helmholtz capacitance of the TiO$_2$/electrolyte interface C (10 μF cm^{-2})[49] and the relation $\Delta Q = C\Delta V$, where ΔV is the change in the conduction band edge potential (10 meV), we estimate ΔQ of -1×10^{-7} C cm^{-2}, which corresponds to the addition of 6×10^{11} cm^{-2} electrons at the surface. On the other hand, assuming that Z907 dye molecules adsorbed at the TiO$_2$ surface result in a downward shift of the TiO$_2$ conduction band edge by 80 mV,[11] we estimate ΔQ

of 8×10^{-7} C cm^{-2}, which corresponds to the addition of 24×10^{11} units of electronic charge per 1 cm^2 of the electrode surface. Therefore, for a 10 mV upward shift of the TiO$_2$ conduction band edge, we have a DINHOP/dye ratio of 1 : 8. Consequently, for 75 μM DINHOP concentration (27 mV upward shift, Fig. 2a), we estimate to have at least 3 negative charges (DINHOP) for every 24 dye molecules.

As far as the decrease of N_{traps} is concerned, an effective upward band shift of 12 mV was calculated using eqn (3), which corresponds to one of every three DINHOP molecules occupying an intra-gap state of TiO$_2$. Additionally, we also infer that, at 375 μM DINHOP concentration (assuming an effective 17 mV upward shift of the TiO$_2$ conduction band edge, Fig. 4), 1 DINHOP molecules per every 12 dye molecules occupy the intra-gap states of the TiO$_2$ surface.

Fig. 5 schematically summarizes the most important findings of the present study. When 75 μM DINHOP is used as a co-adsorbent (Fig. 5a), the DINHOP adsorption at the TiO$_2$ surface leads to: (1) an upward shift of the quasi Fermi level of the TiO$_2$ surface (Fig. 2a) by 27 meV, and (2) about 11% decrease in the total number of intra-gap states at the TiO$_2$ surface (manifested by the increases of both the diffusion coefficient and the recombination rate, Fig. 2b and c). Finally, the upward shift of the conduction band dominates over the decrease of intra-gap states, leading to an effective upward shift of the conduction band edge of around 12 meV, increasing the V_{OC} of DSSCs by about the same amount. It should be noted that for this DINHOP concentration (75 μM), no inhibition of recombination was observed. In contrast, the recombination is increased due to the decrease of intra-gap states (transport-limited recombination process). However, for 750 μM of the co-adsorbent (Fig. 5b), adsorption of DINHOP molecules over the TiO$_2$ surface leads to: (1) a change in its intra-gap state distribution (Fig. 3a), (2) a decrease in the total number of intra-gap states, and (3) a change in the nonlinear recombination order along with a decrease in the charge recombination rate (Fig. 3c). Finally, all these effects lead to an enhancement of V_{OC} of the DSSC by around 34 meV, which is equivalent to an effective upward shift of the conduction band edge of around 35 meV (Fig. 4).

In fact, we assume that there is a direct relationship between the macroscopic and microscopic electronic properties of the TiO$_2$ electrodes on DSSCs. In this direction, thanks to the elemental and orbital selectivity of X-rays used in synchrotron based electronic spectroscopies like X-ray absorption (XAS) and emission (XES) as well as X-ray photoelectron spectroscopy (XPS), it is possible nowadays to investigate the TiO$_2$ electronic states in great detail.[50] Therefore, the energy shifts observed in this work and the variations in the intra-gap states occurring in our and other photovoltaic materials induced by chemical agents and treatments could be experimentally verified by synchrotron based electron spectroscopies.[51,52] Naturally, these spectroscopic techniques are currently being exploited to investigate in great detail the charge transfer mechanism in energy materials under *in situ* and *in operando* conditions.[53] So, incorporation of soft X-ray spectroscopies is necessary to provide direct evidence for our main assumption. We will continue working in this direction.
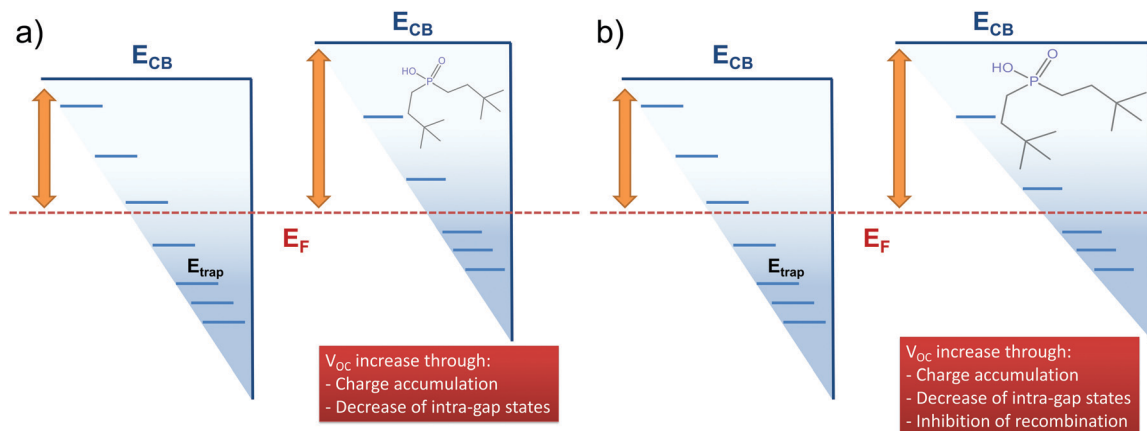
Fig. 5 Schematic representation of the effect of DINHOP adsorption at the surface of TiO$_2$ photoanodes of DSSCs; (a) the combined effect of charge accumulation over the TiO$_2$ surface and a decrease in total intra-gap states, leading to an effective upward shift of the conduction band edge (V_{OC} enhancement); (b) the combined effect of charge accumulation over the TiO$_2$ surface, a decrease in the total intra-gap states and a modification on their distribution, and an inhibition of recombination, leading to an effective upward shift of the conduction band edge (V_{OC} enhancement).

Conclusions

In summary, we investigated the mechanism by which the DINHOP adsorbent affects the open circuit voltage of TiO$_2$ based dye-sensitized solar cells by Stepped Light-Induced Transient Spectroscopy. We demonstrate that the DINHOP (dineohexyl phosphinic acid) co-grafted with Z907 dye onto TiO$_2$ monocrystalline electrodes decreases the intra-gap states at the TiO$_2$ surface. The decrease in intra-gap state density increases both the diffusion coefficient and recombination rate of the charge carriers by a similar fraction. The overall effect of the incorporation of negatively charged DINHOP molecules in the TiO$_2$ photoanode is the upward shift of its conduction band edge towards negative potential. In contrast to the earlier reported results, for most of the used DINHOP concentrations (75 μM and 375 μM), we did not find any evidence of passivation (reduction) of the recombination rate. In contrast, we observed an increase in the carrier recombination rate for all the DINHOP concentrations (compared with the reference DSSC) due to the transport-limited recombination process. Incorporation of DINHOP molecules in higher concentrations (*e.g.* 375 and 750 μM) affects total intra-gap states, their distribution and the nonlinear recombination parameter. However, incorporation of DINHOP molecules in very high concentration (*e.g.* 750 μM) does not significantly affect the position of the quasi Fermi level, rather it inhibits the charge recombination (compared with the 375 μM concentration). The results presented in this work confirm and extend the results of Wang *et al.*[11] and Chandiran *et al.*,[23] who considered similar devices for studying the effect of DINHOP incorporation without electrodynamic consideration. The results of a thorough analysis of the transport and recombination behaviour of electrons interpreted by means of a total electron density model in the DINHOP adsorbed photoanode in the present study are crucial for the better understanding of TiO$_2$ surface charge modification due to the adsorption of co-adsorbents. The procedure utilized to study the electrodynamic behaviour of a co-adsorbent grafted photoanode surface in this work can be easily adapted to study the changes in semiconductor photoanode surfaces due to electrochemical treatment or incorporation of co-adsorbents.

Conflicts of interest

There are no conflicts to declare.

Acknowledgements

References

1 A. Yella, H.-W. Lee, H. N. Tsao, C. Yi, A. K. Chandiran, M. K. Nazeeruddin, E. W.-G. Diau, C.-Y. Yeh, S. M. Zakeeruddin and M. Grätzel, *Science*, 2011, **334**, 629.

2 L. Han, A. Islam, H. Chen, C. Malapaka, B. Chiranjeevi, S. Zhang, X. Yang and M. Yanagida, *Energy Environ. Sci.*, 2012, **5**, 6057–6060.

3 Y. Cao, Y. Liu, S. M. Zakeeruddin, A. Hagfeldt and M. Grätzel, *Joule*, 2018, **2**, 1108–1117.

4 D. Matthews, P. Infelta and M. Grätzel, *Sol. Energy Mater. Sol. Cells*, 1996, **44**, 119–155.

5 G. Smestad, *Sol. Energy Mater. Sol. Cells*, 1994, **32**, 273–288.

6 A. J. Frank, N. Kopidakis and J. V. d. Lagemaat, *Coord. Chem. Rev.*, 2004, **248**, 1165–1179.

7 E. Palomares, J. N. Clifford, S. A. Haque, T. Lutz and J. R. Durrant, *J. Am. Chem. Soc.*, 2003, **125**, 475–482.

8 S. G. Chen, S. Chappel, Y. Diamant and A. Zaban, *Chem. Mater.*, 2001, **13**, 4629–4634.

9 P. Wang, S. M. Zakeeruddin, P. Comte, R. Charvet, R. Humphry-Baker and M. Grätzel, *J. Phys. Chem. B*, 2003, **107**, 14336–14341.

10 P. Wang, S. M. Zakeeruddin, R. Humphry-Baker, J. E. Moser and M. Grätzel, *Adv. Mater.*, 2003, **15**, 2101–2104.

11 M. Wang, X. Li, H. Lin, P. Pechy, S. M. Zakeeruddin and M. Grätzel, *Dalton Trans.*, 2009, 10015–10020, DOI: 10.1039/B908673K,.

12 A. Kay and M. Graetzel, *J. Phys. Chem.*, 1993, **97**, 6272–6277.

13 S. Y. Huang, G. Schlichthörl, A. J. Nozik, M. Grätzel and A. J. Frank, *J. Phys. Chem. B*, 1997, **101**, 2576–2582.

14 G. Schlichthörl, S. Y. Huang, J. Sprague and A. J. Frank, *J. Phys. Chem. B*, 1997, **101**, 8141–8155.

15 S. Rühle, M. Greenshtein, S. G. Chen, A. Merson, H. Pizem, C. S. Sukenik, D. Cahen and A. Zaban, *J. Phys. Chem. B*, 2005, **109**, 18907–18913.

16 N. Kopidakis, N. R. Neale and A. J. Frank, *J. Phys. Chem. B*, 2006, **110**, 12485–12489.

17 N. R. Neale, N. Kopidakis, J. van de Lagemaat, M. Grätzel and A. J. Frank, *J. Phys. Chem. B*, 2005, **109**, 23183–23189.

18 Z. Zhang, S. M. Zakeeruddin, B. C. O'Regan, R. Humphry-Baker and M. Grätzel, *J. Phys. Chem. B*, 2005, **109**, 21818–21824.

19 M. V. Vinayak, T. M. Lakshmykanth, M. Yoosuf, S. Soman and K. R. Gopidas, *Sol. Energy*, 2016, **124**, 227–241.

20 X. Ren, Q. Feng, G. Zhou, C.-H. Huang and Z.-S. Wang, *J. Phys. Chem. C*, 2010, **114**, 7190–7195.

21 C.-P. Lee, C.-T. Li and K.-C. Ho, *Mater. Today*, 2017, **20**, 267–283.

22 T. Marinado, M. Hahlin, X. Jiang, M. Quintana, E. M. J. Johansson, E. Gabrielsson, S. Plogmaker, D. P. Hagberg, G. Boschloo, S. M. Zakeeruddin, M. Grätzel, H. Siegbahn, L. Sun, A. Hagfeldt and H. Rensmo, *J. Phys. Chem. C*, 2010, **114**, 11903–11910.

23 A. K. Chandiran, S. M. Zakeeruddin, R. Humphry-Baker, M. K. Nazeeruddin, M. Grätzel and F. Sauvage, *ChemPhysChem*, 2017, **18**, 2724–2731.

24 V. Sugathan, E. John and K. Sudhakar, *Renewable Sustainable Energy Rev.*, 2015, **52**, 54–64.

25 A. Błaszczyk, *Dyes Pigm.*, 2018, **149**, 707–718.

26 J. Villanueva-Cab, J. A. Anta and G. Oskam, *Phys. Chem. Chem. Phys.*, 2016, **18**, 2303–2308.

27 S. Nakade, T. Kanzaki, Y. Wada and S. Yanagida, *Langmuir*, 2005, **21**, 10803–10807.

28 J. A. Anta, J. Idígoras, E. Guillén, J. Villanueva-Cab, H. J. Mandujano-Ramírez, G. Oskam, L. Pellejà and E. Palomares, *Phys. Chem. Chem. Phys.*, 2012, **14**, 10285–10299.

29 K. Zhu, N. R. Neale, A. F. Halverson, J. Y. Kim and A. J. Frank, *J. Phys. Chem. C*, 2010, **114**, 13433–13441.

30 J. van de Lagemaat, N. Kopidakis, N. R. Neale and A. J. Frank, *Phys. Rev. B: Condens. Matter Mater. Phys.*, 2005, **71**, 035304.

31 J. Bisquert, *J. Phys. Chem. B*, 2004, **108**, 2323–2332.

32 Y. Wang, D. Wu, L.-M. Fu, X.-C. Ai, D. Xu and J.-P. Zhang, *Phys. Chem. Chem. Phys.*, 2014, **16**.

33 D. Pourjafari, D. Reyes-Coronado, A. Vega-Poot, R. Escalante, D. Kirkconnell-Reyes, R. García-Rodríguez, J. A. Anta and G. Oskam, *J. Phys. Chem. C*, 2018, **122**, 14277–14288.

34 K. Zhu, N. Kopidakis, N. R. Neale, J. van de Lagemaat and A. J. Frank, *J. Phys. Chem. B*, 2006, **110**, 25174–25180.

35 J. Nelson, S. A. Haque, D. R. Klug and J. R. Durrant, *Phys. Rev. B: Condens. Matter Mater. Phys.*, 2001, **63**, 205321.

36 N. Kopidakis, N. R. Neale, K. Zhu, J. van de Lagemaat and A. J. Frank, *Appl. Phys. Lett.*, 2005, **87**, 202106.

37 N. Kopidakis, E. A. Schiff, N. G. Park, J. van de Lagemaat and A. J. Frank, *J. Phys. Chem. B*, 2000, **104**, 3930–3936.

38 N. Kopidakis, K. D. Benkstein, J. van de Lagemaat, A. J. Frank, Q. Yuan and E. A. Schiff, *Phys. Rev. B: Condens. Matter Mater. Phys.*, 2006, **73**, 045326.

39 N. Kopidakis, K. D. Benkstein, J. van de Lagemaat and A. J. Frank, *J. Phys. Chem. B*, 2003, **107**, 11307–11315.

40 K. D. Benkstein, N. Kopidakis, J. van de Lagemaat and A. J. Frank, *J. Phys. Chem. B*, 2003, **107**, 7759–7767.

41 F. Cao, G. Oskam, G. J. Meyer and P. C. Searson, *J. Phys. Chem.*, 1996, **100**, 17021–17027.

42 P. E. de Jongh and D. Vanmaekelbergh, *Phys. Rev. Lett.*, 1996, **77**, 3427–3430.

43 G. Schlichthörl, N. G. Park and A. J. Frank, *J. Phys. Chem. B*, 1999, **103**, 782–791.

44 L. Dloczik, O. Ileperuma, I. Lauermann, L. M. Peter, E. A. Ponomarev, G. Redmond, N. J. Shaw and I. Uhlendorf, *J. Phys. Chem. B*, 1997, **101**, 10281–10289.

45 A. Solbrand, H. Lindström, H. Rensmo, A. Hagfeldt, S.-E. Lindquist and S. Södergren, *J. Phys. Chem. B*, 1997, **101**, 2514–2518.

46 J. van de Lagemaat and A. J. Frank, *J. Phys. Chem. B*, 2001, **105**, 11194–11205.

47 J. Nelson, *Phys. Rev. B: Condens. Matter Mater. Phys.*, 1999, **59**, 15374–15380.

48 J. Villanueva-Cab, S.-R. Jang, A. F. Halverson, K. Zhu and A. J. Frank, *Nano Lett.*, 2014, **14**, 2305–2309.

49 J. van de Lagemaat, N. G. Park and A. J. Frank, *J. Phys. Chem. B*, 2000, **104**, 2044–2052.

50 d. G. Frank and K. Akio, *Core Level Spectroscopy of Solids*, 2008.

51 S. Benkoula, O. Sublemontier, M. Patanen, C. Nicolas, F. Sirotti, A. Naitabdi, F. Gaie-Levrel, E. Antonsson, D. Aureau, F.-X. Ouf, S.-I. Wada, A. Etcheberry, K. Ueda and C. Miron, *Sci. Rep.*, 2015, **5**, 15088.

52 J. Villanueva-Cab, P. Olalde-Velasco, A. Romero-Contreras, Z. Zhuo, F. Pan, S. E. Rodil, W. Yang and U. Pal, *ACS Appl. Mater. Interfaces*, 2018, **10**, 31374–31383.

53 X. Liu, W. Yang and Z. Liu, *Adv. Mater.*, 2014, **26**, 7710–7729.